Author(s): Muscolino, G. and Palmeri, A.

Title: An earthquake response spectrum method for linear light secondary substructures

Publication year: 2007

Journal title: ISET Journal of Earthquake Technology

ISSN: 0972-0405

Publisher: Indian Society for Earthquake Technology

Publisher's site: *http://www.iitr.ernet.in/iset/*

Link to original published version: N/A

"An earthquake response spectrum method for linear light secondary substructures"

by

Giuseppe MUSCOLINO & Alessandro PALMERI

AN EARTHQUAKE RESPONSE SPECTRUM METHOD
FOR LINEAR LIGHT SECONDARY SUBSTRUCTURES

by Giuseppe Muscolino[*] and Alessandro Palmeri[†]

ABSTRACT

The earthquake response spectrum is the most popular tool in the seismic analysis and design of structures. In the case of combined Primary-Secondary (P-S) systems, the response of the supporting P substructure is generally evaluated without considering the S substructure, which in turn is only required to bear displacements and/or forces imposed by the P one ("cascade" approach). In doing so, however, the dynamic interaction among P and S components is neglected, and the seismic-induced response of the S substructure may be heavily underestimated or overestimated. In this paper, a novel CQC (Complete Quadratic Combination) rule is proposed for the seismic response of linear light S substructures attached to linear P substructures. The proposed technique overcomes the drawbacks of the cascade approach by including the effects of dynamic interaction and different damping in the substructures directly in the cross-correlation coefficients. The computational effort is reduced by using the eigenproperties of the decoupled substructures and only one earthquake response spectrum for a reference value of the damping ratio.

[*] Corresponding Author. Professor, Department of Civil Engineering, University of Messina. Vill. S. Agata, 98166, Messina, Italy. Telephone +39 090 397 7159, Fax +39 090 397 7480, Email <muscolin@ingegneria.unime.it>.

[†] Research Fellow and Adjunct Professor, Department of Civil Engineering, University of Messina. Vill. S. Agata, 98166, Messina, Italy. Telephone +39 090 397 7170, Fax +39 090 397 7480, Email <alexpalm@ingegneria.unime.it>.

INTRODUCTION

Although not part of the Primary (P) load-bearing structural system, the seismic analysis and design of light Secondary (S) attachments to buildings or industrial facilities is a topic of broad engineering interest (among others, Chen and Soong, 1988; Singh, 1988; Villaverde, 2004; Singh at al., 2006a and b; and references provided therein). Past experiences, in fact, prove that S substructures such as suspended ceilings and non-structural walls, piping systems and antennas, storage tanks and electrical transformers must survive earthquakes in order to facilitate emergency and recovery services in the aftermath and avoid direct and/or indirect human and/or economical losses. On the other hand, some special dynamic properties make S substructures particularly vulnerable to earthquakes. First of all, S substructures are usually much lighter than the P substructure to which they are attached, and the stiffness of S components (including anchors) is much smaller than the stiffness of P components: as a result, in most of the real cases the modal frequencies of S substructures are close to (and some times tuned to) those of the P substructure. Moreover, the vibration of the P substructure tends to amplify the effects of the ground motion on the S substructures, principally on those attached at the top (e.g., antennas). In addition, the damping capabilities of S attachments are generally much smaller than those of the P supporting system, and so the resonance phenomenon may occur.

The above considerations would suggest the use of rigorous approaches, in which the dynamic interaction among P and S substructures is fully accounted for. In practical applications, however, combined P-S systems have an excessive number of degrees of freedom and show large differences in the mass, stiffness and damping coefficients. Therefore, conventional methods, such as modal analysis with the earthquake response spectrum and time history analysis with recorded and/or generated accelerograms, may become too expensive and inaccurate. Conversely, the so-called "cascade" approximation, in which the feedback of the S substructures on the P one is neglected, even though very popular, may be too simplistic. In this approach, in fact, P and S substructures are decoupled and analysed in sequence (e.g., Falsone et al., 1991; Lavelle et al., 1991): in the first stage, the seismic response of the P substructure is evaluated neglecting the presence of any S

substructure; in the second stage, the dynamic response of each S substructure is evaluated considering the motion of the P substructure at the anchor points, other than the ground motion. Unfortunately, in a number of real cases this approach may lead to inaccurate predictions, e.g. when the effect of spatial coupling is significant.

In this paper, the concept of "Light Secondary Substructure" (LSS) approximation is stressed, and the limits of validity are investigated with reference to a simple 2-DoF combined P-S system. This approximation is used in deriving a novel CQC (Complete Quadratic Combination) rule, which can be viewed as a special variant of the method recently formulated by Falsone and Muscolino (1999 and 2004) for the seismic analysis of non-classically damped structures. For the validation purposes, numerical results are presented in the simplest case where the new combination coefficients are consistent with the assumption of white noise excitation, while the formulation can be easily extended to any Power Spectral Density (PSD) function of the seismic input. Among the advantages of the proposed approach: i) the eigenproperties involved in the computations (modal frequencies and modal shapes) are those of the decoupled substructures, assumed to be fixed to their own bases; ii) the cross-correlation coefficients incorporate the effects of frequency tuning and different damping in the substructures; iii) just a single earthquake response spectrum, for a reference value of the viscous damping ratio, is required. The latter feature of the proposed approach is probably the most important one. Methods based on the direct characterization of the seismic hazard by the PSD of the ground acceleration, in fact, enable to account for the dynamic interaction among P and S substructures through the appropriate definition of the Frequency Response Function (FRF) of the combined P-S system, for which the individual base-fixed modal properties can be used (Dey and Gupta, 1999). However, to date, the PSD function is considered almost exclusively in the academic community and for studying structures of exceptional importance. Seventy-five years after the pioneering work by Professor Maurice Biot (1932, 1933, 1934), thus, the earthquake response spectrum is still the most popular tool for the analysis and design of conventional earthquake-resistant structures. Given its extreme simplicity, moreover, a number of deterministic and stochastic extensions has been proposed in the literature. Among others, Amini and Trifunac (1985) developed a stochastic method for

estimating not just the largest, but all the ordered peaks of the seismic response of linear structures; this method has been refined by Gupta and Trifunac (1988), and can be useful in order to better understand the progressive damage under successive excursions of the seismic response beyond a certain design level; Gupta and Trifunac (1989) formulated a probabilistic extension which takes into account the rotational components of the ground motion along with the translational components; the effects of wave passage, loss of coherency with distance and variation of local soil conditions are included in the method proposed by Der Kiureghian and Neuenhofer (1992) for the seismic analysis of multiply-supported structures subjected to spatially-varying ground motions; Iwan (1997) proposed a new earthquake drift spectrum based on a continuous shear-beam model rather than a Single-Degree-of-Freedom oscillator, which proves to give important information for near-source pulse-like ground shakings. From this point of view, then, the main intend of CQC rule proposed in this paper could be claimed to be the attempt of extending to light secondary attachments the original statement by Professor Maurice Biot (1933) that "the maximum effect of earthquakes on buildings will be easily evaluated…"

EQUATIONS OF MOTION

In this section, the equations of motion of a Primary (P) structural system, with n_P DoFs (Degrees of Freedom), connected to a lighter Secondary (S) attachment, with n_S DoFs, are established in the linear range. In the following, the damping of both P and S substructures is assumed to be linear hysteretic (among others, Nashif et al., 1985; Inaudi and Kelly, 1995; Muscolino et al., 2005; and references provided therein). Experimental analyses, in fact, demonstrate that in most of the cases the dissipation of engineering materials is nearly frequency-independent. This means that, ideally, the damping forces are proportional to the strains, but in phase with the strain rates. This behaviour can be easily introduced in the frequency domain, while much more complicated is the application in the time domain (Makris, 1997; Makris and Zhang, 2000; Muscolino et al., 2005), and for this reason the linear viscous damping is usually preferred in Structural Dynamics. When combined P-S systems are dealt with, however, the formation of the viscous damping matrix is not straightforward

(e.g., Gupta and Jaw, 1986; Muscolino, 1990; Feriani and Perotti, 1996), and the use of the linear hysteretic damping is preferable.

Combined P-S system

In the mixed time-frequency domain, the seismic motion of the combined P-S system shown in Figure 1 is ruled by:

$$\mathbf{M}\,\ddot{\mathbf{u}}(t)+\mathbf{K}(\omega)\,\mathbf{u}(t)=-\mathbf{M}\,\boldsymbol{\tau}\,\ddot{u}_{\mathrm{g}}(t) \tag{1}$$

where $\mathbf{u}(t)=\begin{bmatrix}\mathbf{u}_{\mathrm{S}}^{\mathrm{T}}(t) & \mathbf{u}_{\mathrm{P}}^{\mathrm{T}}(t)\end{bmatrix}^{\mathrm{T}}$ is the $n\times1$ array ($n=n_{\mathrm{S}}+n_{\mathrm{P}}$) which collects the DoFs (total displacements), in which those of the P substructure, listed in the array $\mathbf{u}_{\mathrm{P}}(t)$, are appended to the DoFs of the S substructure, listed in the array $\mathbf{u}_{\mathrm{S}}(t)$; $\ddot{u}_{\mathrm{g}}(t)$ is the time history of the ground acceleration and $\boldsymbol{\tau}$ is its influence vector, whose elements can be partitioned as $\boldsymbol{\tau}=\begin{bmatrix}\boldsymbol{\tau}_{\mathrm{S}}^{\mathrm{T}} & \boldsymbol{\tau}_{\mathrm{P}}^{\mathrm{T}}\end{bmatrix}^{\mathrm{T}}$; $\mathbf{M}$ and $\mathbf{K}(\omega)$ are the matrix of inertia and the complex-valued dynamic stiffness matrix, respectively; and where, as usual, the over-dot means time derivative. The matrices $\mathbf{M}$ and $\mathbf{K}(\omega)$ can be partitioned as:

$$
\mathbf{M}=\begin{bmatrix}\mathbf{M}_{\mathrm{S}} & \mathbf{0} \\ \hline \mathbf{0} & \mathbf{M}_{\mathrm{P}}\end{bmatrix}
$$
$$
\mathbf{K}(\omega)=\begin{bmatrix}\mathbf{K}_{\mathrm{S}}\times\left[1+\mathrm{j}\eta_{\mathrm{S}}\,\mathrm{sign}(\omega)\right] & \mathbf{0} \\ \hline \mathbf{0} & \mathbf{K}_{\mathrm{P}}\times\left[1+\mathrm{j}\eta_{\mathrm{P}}\,\mathrm{sign}(\omega)\right]\end{bmatrix}+\begin{bmatrix}\mathbf{0} & \mathbf{K}_{\mathrm{SP}} \\ \hline \mathbf{K}_{\mathrm{SP}}^{\mathrm{T}} & \Delta\mathbf{K}_{\mathrm{P}}\end{bmatrix}\times\left[1+\mathrm{j}\eta_{\mathrm{S}}\,\mathrm{sign}(\omega)\right] \tag{2}
$$

where the real-valued mass and stiffness matrices of the S substructure, $\mathbf{M}_{\mathrm{S}}$ and $\mathbf{K}_{\mathrm{S}}$, and of the P substructure, $\mathbf{M}_{\mathrm{P}}$ and $\mathbf{K}_{\mathrm{P}}$, are those assembled under the assumption to be fixed to their own bases: that is, the P substructure is fixed to the ground (Fig. 2a), while the S substructure is fixed to the support points on the P substructure as well as to the ground (Fig. 2b); $\mathbf{K}_{\mathrm{SP}}$ is the stiffness matrix coupling the P and S substructures, while $\Delta\mathbf{K}_{\mathrm{P}}$ is the increment in the stiffness matrix of the P substructure due to the presence of the S substructure; and where η_{S} and η_{P} are the loss factors of the S and of the P substructures, respectively, while $\mathrm{j}=\sqrt{-1}$ is the imaginary unit and ω is the vibration frequency.

The seismic response of the coupled P-S system is given in the frequency domain by:

$$\text{F}\langle \mathbf{u}(t) \rangle = \mathbf{H}(\omega)\,\text{F}\langle \ddot{u}_{\text{g}}(t) \rangle \tag{3}$$

where the symbol $\text{F}\langle \cdot \rangle$ stands for the Fourier Transform operator, and $\mathbf{H}(\omega)$ is the $n \times 1$ array listing the Frequency Response Functions (FRFs) of the DoFs:

$$\mathbf{H}(\omega) = -\left[\mathbf{M}^{-1}\mathbf{K}(\omega) - \omega^2 \mathbf{I}_n \right]^{-1} \boldsymbol{\tau}$$

$\mathbf{I}_n$ being the $n \times n$ identity matrix.

Modal transformations

The dynamic response of the combined P-S system can be conveniently represented in the reduced modal space by means of the so-called "admissible coordinate transformation" (Muscolino, 1990), given by:

$$\mathbf{u}(t) = \boldsymbol{\Gamma}\,\mathbf{q}(t) \tag{4}$$

where $\mathbf{q}(t) = \left[\mathbf{q}_{\text{S}}^{\text{T}}(t) \mid \mathbf{q}_{\text{P}}^{\text{T}}(t) \right]^{\text{T}}$ is the $m \times 1$ array ($m = m_{\text{S}} + m_{\text{P}} \le n$) listing the modal coordinates of the combined P-S system, in which the array of the $m_{\text{P}} \le n_{\text{P}}$ modal coordinates of the P substructure, $\mathbf{q}_{\text{P}}(t)$, is appended to the array of the $m_{\text{S}} \le n_{\text{S}}$ modal coordinates of the S substructure, $\mathbf{q}_{\text{S}}(t)$; and where $\boldsymbol{\Gamma}$ is the transformation matrix, which is partitioned as:

$$\boldsymbol{\Gamma} = \left[\begin{array}{c|c} \boldsymbol{\Phi}_{\text{S}} & \boldsymbol{\Psi}_{\text{SP}} \\ \hline \mathbf{0} & \boldsymbol{\Phi}_{\text{P}} \end{array} \right] \tag{5}$$

$\boldsymbol{\Phi}_{\text{S}} = \left[\boldsymbol{\phi}_{\text{S1}} \quad \cdots \quad \boldsymbol{\phi}_{\text{S}m_{\text{S}}} \right]$ and $\boldsymbol{\Phi}_{\text{P}} = \left[\boldsymbol{\phi}_{\text{P1}} \quad \cdots \quad \boldsymbol{\phi}_{\text{P}m_{\text{P}}} \right]$ being the modal matrices of the S and P substructures, of dimensions $n_{\text{S}} \times m_{\text{S}}$ and $n_{\text{P}} \times m_{\text{P}}$, respectively, whose columns are the modal shapes of the two base-fixed substructures (Figs. 3a and b); while $\boldsymbol{\Psi}_{\text{SP}} = \left[\boldsymbol{\psi}_{\text{SP1}} \quad \cdots \quad \boldsymbol{\psi}_{\text{SP}m_{\text{S}}} \right]$ is the modal coupling matrix, of dimensions $n_{\text{S}} \times m_{\text{P}}$, whose columns are the deformed shapes of the S substructure due to the displacements at the support points for the modal shapes of the P substructure (Fig. 3c). The modal matrices $\boldsymbol{\Phi}_{\text{S}}$ and $\boldsymbol{\Phi}_{\text{P}}$ can be evaluated by solving the classical eigenproblems:

$$\mathbf{M}_{\text{S}}\,\boldsymbol{\Phi}_{\text{S}}\,\boldsymbol{\Omega}_{\text{S}}^2 = \mathbf{K}_{\text{S}}\,\boldsymbol{\Phi}_{\text{S}} \quad ; \quad \mathbf{M}_{\text{P}}\,\boldsymbol{\Phi}_{\text{P}}\,\boldsymbol{\Omega}_{\text{P}}^2 = \mathbf{K}_{\text{P}}\,\boldsymbol{\Phi}_{\text{P}} \tag{6}$$

$\mathbf{\Omega}_{\mathrm{S}} = \mathrm{diag}\left\{\omega_{\mathrm{S}1}, \cdots, \omega_{\mathrm{S}m_{\mathrm{S}}}\right\}$ and $\mathbf{\Omega}_{\mathrm{P}} = \mathrm{diag}\left\{\omega_{\mathrm{P}1}, \cdots, \omega_{\mathrm{P}m_{\mathrm{P}}}\right\}$ being the spectral matrices of the S and P substructures, respectively, whose elements are the undamped modal circular frequencies of the two base-fixed substructures; while the modal coupling matrix $\mathbf{\Psi}_{\mathrm{SP}}$ is given by:

$$\mathbf{\Psi}_{\mathrm{SP}} = \mathbf{N}_{\mathrm{SP}}\,\mathbf{\Phi}_{\mathrm{P}} \quad ; \quad \mathbf{N}_{\mathrm{SP}} = -\mathbf{K}_{\mathrm{S}}^{-1}\,\mathbf{K}_{\mathrm{SP}}$$

$\mathbf{N}_{\mathrm{SP}}$ being the so-called pseudo-static influence matrix of the P substructure on the S one. Upon substitution of Eq. (4) into Eq. (1), one obtains:

$$\mathbf{m}\,\ddot{\mathbf{q}}(t) + \mathbf{k}(\omega)\,\mathbf{q}(t) = \mathbf{g}\,\ddot{u}_{\mathrm{g}}(t) \tag{7}$$

where the symmetric matrices $\mathbf{m}$ and $\mathbf{k}(\omega)$ are the matrix of inertia and the complex-valued dynamic stiffness matrix in the reduced modal space, respectively, while $\mathbf{g}$ is the modal influence vector of the seismic input. These quantities take the expressions:

$$\mathbf{m} = \mathbf{\Gamma}^{\mathrm{T}}\mathbf{M}\mathbf{\Gamma} = \left[\begin{array}{c|c} \mathbf{I}_{m_{\mathrm{S}}} & \mathbf{m}_{\mathrm{SP}} \\ \hline \mathbf{m}_{\mathrm{SP}}^{\mathrm{T}} & \mathbf{I}_{m_{\mathrm{P}}} + \Delta\mathbf{m}_{\mathrm{P}} \end{array}\right]$$

$$\mathbf{k}(\omega) = \mathbf{\Gamma}^{\mathrm{T}}\mathbf{K}(\omega)\mathbf{\Gamma} = \left[\begin{array}{c|c} \mathbf{\Omega}_{\mathrm{S}}^{2}\,\gamma(\omega) & \mathbf{0} \\ \hline \mathbf{0} & \mathbf{\Omega}_{\mathrm{P}}^{2} + \Delta\mathbf{k}_{\mathrm{P}}\,\gamma(\omega) \end{array}\right] \times \left[1 + \mathrm{j}\eta_{\mathrm{P}}\,\mathrm{sign}(\omega)\right] \tag{8}$$

$$\mathbf{g} = -\mathbf{\Gamma}^{\mathrm{T}}\mathbf{M}\,\mathbf{\tau} = -\left[\begin{array}{c} \mathbf{p}_{\mathrm{S}} \\ \hline \mathbf{p}_{\mathrm{P}} + \Delta\mathbf{p}_{\mathrm{P}} \end{array}\right]$$

where the out-of-diagonal term $\mathbf{m}_{\mathrm{SP}}$ in the matrix of inertia is defined by:

$$\mathbf{m}_{\mathrm{SP}} = \mathbf{\Phi}_{\mathrm{S}}^{\mathrm{T}}\,\mathbf{M}_{\mathrm{S}}\,\mathbf{\Psi}_{\mathrm{SP}}$$

$\mathbf{p}_{\mathrm{S}}$ and $\mathbf{p}_{\mathrm{P}}$ are the arrays listing the usual modal participation factors of the P and S substructures, respectively:

$$\mathbf{p}_{\mathrm{S}} = \mathbf{\Phi}_{\mathrm{S}}^{\mathrm{T}}\,\mathbf{M}_{\mathrm{S}}\,\mathbf{\tau}_{\mathrm{S}} \quad ; \quad \mathbf{p}_{\mathrm{P}} = \mathbf{\Phi}_{\mathrm{P}}^{\mathrm{T}}\,\mathbf{M}_{\mathrm{P}}\,\mathbf{\tau}_{\mathrm{P}} \tag{9}$$

the increments $\Delta\mathbf{m}_{\mathrm{P}}$, $\Delta\mathbf{k}_{\mathrm{P}}$ and $\Delta\mathbf{p}_{\mathrm{P}}$ are given by:

$$\Delta\mathbf{m}_{\mathrm{P}} = \mathbf{\Psi}_{\mathrm{SP}}^{\mathrm{T}}\,\mathbf{M}_{\mathrm{S}}\,\mathbf{\Psi}_{\mathrm{SP}} \quad ; \quad \Delta\mathbf{k}_{\mathrm{P}} = \mathbf{\Phi}_{\mathrm{P}}^{\mathrm{T}}\left(\Delta\mathbf{K}_{\mathrm{P}} + \mathbf{K}_{\mathrm{SP}}^{\mathrm{T}}\,\mathbf{N}_{\mathrm{SP}}\right)\mathbf{\Phi}_{\mathrm{P}}$$

$$\Delta\mathbf{p}_{\mathrm{P}} = \mathbf{\Phi}_{\mathrm{P}}^{\mathrm{T}}\,\mathbf{N}_{\mathrm{SP}}^{\mathrm{T}}\,\mathbf{M}_{\mathrm{S}}\,\mathbf{\tau}_{\mathrm{S}}$$

while $\gamma(\omega)$ is a complex-valued function that accounts for the different damping in the substructures:

$$\gamma(\omega) = \frac{1 + j\eta_S \operatorname{sign}(\omega)}{1 + j\eta_P \operatorname{sign}(\omega)} = \frac{(1 + \eta_S \eta_P) + j(\eta_S - \eta_P)\operatorname{sign}(\omega)}{1 + \eta_P^2}$$

According to Eqs. (4) and (8), the seismic response of the coupled P-S system can be evaluated in the frequency domain as:

$$F\langle \mathbf{u}(t) \rangle = \mathbf{\Gamma}\,\mathbf{h}(\omega)\,F\langle \ddot{u}_g(t) \rangle \tag{10}$$

where $\mathbf{h}(\omega)$ is the $m \times 1$ array listing the modal FRFs:

$$\mathbf{h}(\omega) = \left[\mathbf{k}(\omega) - \omega^2\,\mathbf{m} \right]^{-1} \mathbf{g} = \left[\mathbf{A}(\omega) - \omega^2\,\mathbf{I}_m \right]^{-1} \mathbf{b}$$

in which:

$$\mathbf{A}(\omega) = \mathbf{m}^{-1}\,\mathbf{k}(\omega) \quad ; \quad \mathbf{b} = \mathbf{m}^{-1}\,\mathbf{g} \tag{11}$$

APPROXIMATE RESPONSE OF A SIMPE 2-DOF COMBINED P-S SYSTEM

In this section, the simplest case in which both P and S substructures are single-DoF oscillators is considered, with the aim of investigating the effects that two different approximations, namely the "Light Secondary Substructure" (LSS) approximation and the "cascade" approximation, may have on the seismic response of the combined P-S system. This analysis reveals what terms are negligible when the S substructure is much lighter that the P one, and these results are extended in the next section to the general case in which both P and S substructures are multi-DoF systems.

With reference to the combined P-S system depicted in Figure 4a, the matrices $\mathbf{M}$ and $\mathbf{K}(\omega)$ in Eqs. (2) simplifies as:

$$\mathbf{M} = \begin{bmatrix} M_S & 0 \\ \hline 0 & M_P \end{bmatrix}$$

$$\mathbf{K}(\omega) = \begin{bmatrix} K_S \gamma(\omega) & -\dfrac{K_S}{2}\gamma(\omega) \\ \hline -\dfrac{K_S}{2}\gamma(\omega) & K_P + \dfrac{K_S}{2}\gamma(\omega) \end{bmatrix} \times \left[1 + j\eta_P \operatorname{sign}(\omega)\right] \tag{12}$$

while $\mathbf{u}(t) = \left[u_S(t) \mid u_P(t)\right]^T$ and $\boldsymbol{\tau} = \left[1 \mid 1\right]^T$. After some algebra, one can prove that the transformation matrix $\boldsymbol{\Gamma}$ consistent with Eq. (5) is:

$$\boldsymbol{\Gamma} = \begin{bmatrix} M_S^{-1/2} & \dfrac{1}{2}M_P^{-1/2} \\ \hline 0 & M_P^{-1/2} \end{bmatrix}$$

The modal quantities in Eqs. (8), then, take the expressions:

$$\mathbf{m} = \begin{bmatrix} 1 & \dfrac{\sqrt{\alpha}}{2} \\ \hline \dfrac{\sqrt{\alpha}}{2} & 1 + \dfrac{\alpha}{4} \end{bmatrix} \quad ; \quad \mathbf{k}(\omega) = \omega_P^2 \times \begin{bmatrix} \beta^2 \gamma(\omega) & 0 \\ \hline 0 & 1 + \dfrac{\alpha \beta^2 \gamma(\omega)}{4} \end{bmatrix} \times \left[1 + j\eta_P \operatorname{sign}(\omega)\right]$$

$$\mathbf{g} = -\begin{bmatrix} \dfrac{\sqrt{\alpha}}{1 + \dfrac{\alpha}{2}} \end{bmatrix} \tag{13}$$

where α is the mass ratio and β is a tuning parameter:

$$\alpha = \frac{M_S}{M_P} \quad ; \quad \beta = \frac{\omega_S}{\omega_P} \tag{14}$$

ω_P and ω_S being the undamped natural circular frequencies of the P (Fig. 4b) and S (Fig. 4c) oscillators:

$$\omega_P = \sqrt{\frac{K_P}{M_P}} \quad ; \quad \omega_S = \sqrt{\frac{K_S}{M_S}} \tag{15}$$

LSS approximation

When the S substructure is light with respect to the P one, i.e. $M_S \ll M_P$, the mass ratio (first of Eq. (14)) is much less than one, i.e. $\alpha \ll 1$. Accordingly, this term can be neglected in the dynamic stiffness matrix and in the influence vector given in Eqs. (13):

$$\hat{\mathbf{k}}(\omega) = \omega_P^2 \times \left[\begin{array}{c|c} \beta^2\,\gamma(\omega) & 0 \\ \hline 0 & 1 \end{array} \right] \times \left[1 + j\eta_P \operatorname{sign}(\omega) \right] \quad ; \quad \hat{\mathbf{g}} = -\left[\begin{array}{c} \sqrt{\alpha} \\ \hline 1 \end{array} \right] \tag{16}$$

Additionally, in the complex-valued modal stiffness matrix $\hat{\mathbf{k}}(\omega)$ (first of Eqs. (16)) it is assumed that $\left| \alpha\,\beta^2\,\gamma(\omega) \right| \ll 1$. In practical applications, in fact, $\left| \gamma(\omega) \right| \cong 1$, while from Eqs. (14) and (15) it follows that the stiffness ratio K_S/K_P is given by $\alpha\,\beta^2$, and this ratio needs to much less than one in order the "secondary" stiffness K_S to be negligible with respect to the "primary" stiffness K_P. Upon substitution of Eqs. (16) into Eqs. (11), one obtains for the proposed LSS approximation:

$$\hat{\mathbf{A}}(\omega) = \mathbf{m}^{-1}\,\hat{\mathbf{k}}(\omega) = \omega_P^2 \times \left[\begin{array}{c|c} \left(1+\dfrac{\alpha}{4}\right)\beta^2\,\gamma(\omega) & -\dfrac{\sqrt{\alpha}}{2} \\ \hline -\dfrac{\sqrt{\alpha}}{2}\,\beta^2\,\gamma(\omega) & 1 \end{array} \right] \times \left[1 + j\eta_P \operatorname{sign}(\omega) \right]$$

$$\hat{\mathbf{b}} = \mathbf{m}^{-1}\,\hat{\mathbf{g}} = -\left[\begin{array}{c} \dfrac{\dfrac{\sqrt{\alpha}}{2}+\dfrac{\alpha\sqrt{\alpha}}{4}}{1-\dfrac{\alpha}{2}} \end{array} \right] \cong -\left[\begin{array}{c} \dfrac{\sqrt{\alpha}}{2} \\ \hline 1 \end{array} \right] \tag{17}$$

being:

$$\mathbf{m}^{-1} = \left[\begin{array}{c|c} 1+\dfrac{\alpha}{4} & -\dfrac{\sqrt{\alpha}}{2} \\ \hline -\dfrac{\sqrt{\alpha}}{2} & 1 \end{array} \right] \tag{18}$$

The approximate array of the modal FRFs, then, can be evaluated as:

$$\hat{\mathbf{h}}(\omega) = \left[\hat{\mathbf{A}}(\omega) - \omega^2\,\mathbf{I}_2 \right]^{-1} \hat{\mathbf{b}} = \left[\begin{array}{c} \hat{h}_S(\omega) \\ \hline \hat{h}_P(\omega) \end{array} \right] \tag{19}$$

10

where $\hat{h}_{\mathrm{S}}(\omega)$ and $\hat{h}_{\mathrm{P}}(\omega)$ are the approximate FRFs of the modal coordinates of S oscillator, $q_{\mathrm{S}}(t) = \sqrt{M_{\mathrm{S}}}\left[u_{\mathrm{S}}(t) - u_{\mathrm{P}}(t)/2\right]$, and P oscillator, $q_{\mathrm{P}}(t) = \sqrt{M_{\mathrm{P}}}\,u_{\mathrm{P}}(t)$, respectively. The comparison between Eqs. (3) and (10), finally, gives the array of the corresponding FRFs of the DoFs $u_{\mathrm{S}}(t)$ and $u_{\mathrm{P}}(t)$, in that order:

$$\hat{\mathbf{H}}(\omega) = \mathbf{\Gamma}\,\hat{\mathbf{h}}(\omega) = \begin{bmatrix} M_{\mathrm{S}}^{-1/2}\,\hat{h}_{\mathrm{S}}(\omega) + \dfrac{1}{2} M_{\mathrm{P}}^{-1/2}\,\hat{h}_{\mathrm{P}}(\omega) \\ \noalign{\vskip2pt}\hline\noalign{\vskip2pt} M_{\mathrm{P}}^{-1/2}\,\hat{h}_{\mathrm{P}}(\omega) \end{bmatrix} \tag{20}$$

Cascade approximation

When the S substructure is much lighter than the P substructure, i.e. $\alpha \ll 1$, the dynamic interaction in the coupled P-S system is often ignored, and the seismic responses of the P and S substructures are evaluated in cascade. Accordingly, in a first stage the response of the P substructure to the ground motion is computed by neglecting the feedback of the S one, while in a second stage the response of the S substructure is computed by taking into account both the response of the P one and the seismic input. As a result, the dynamic stiffness matrix $\mathbf{K}(\omega)$ in the second of Eqs. (12) becomes asymmetric, since the lower out-of-diagonal term goes to zero:

$$\bar{\mathbf{K}}(\omega) = \begin{bmatrix} K_{\mathrm{S}}\left[1 + \mathrm{j}\eta_{\mathrm{S}}\,\mathrm{sign}(\omega)\right] & -\dfrac{K_{\mathrm{S}}}{2}\left[1 + \mathrm{j}\eta_{\mathrm{S}}\,\mathrm{sign}(\omega)\right] \\ \noalign{\vskip2pt}\hline\noalign{\vskip2pt} 0 & K_{\mathrm{P}}\left[1 + \mathrm{j}\eta_{\mathrm{P}}\,\mathrm{sign}(\omega)\right] \end{bmatrix}$$

and the approximate array of the FRFs of the DoFs takes the form:

$$\bar{\mathbf{H}}(\omega) = -\left[\mathbf{M}^{-1}\bar{\mathbf{K}}(\omega) - \omega^2\,\mathbf{I}_n\right]^{-1}\boldsymbol{\tau}$$

$$= \begin{bmatrix} \dfrac{\omega^2 - \left[1 + \dfrac{\beta^2\,\gamma(\omega)}{2}\right]\omega_{\mathrm{P}}^2\left[1 + \mathrm{j}\eta_{\mathrm{P}}\,\mathrm{sign}(\omega)\right]}{\left\{\omega^2 - \beta^2\,\omega_{\mathrm{S}}^2\left[1 + \mathrm{j}\eta_{\mathrm{S}}\,\mathrm{sign}(\omega)\right]\right\}\left\{\omega^2 - \omega_{\mathrm{P}}^2\left[1 + \mathrm{j}\eta_{\mathrm{P}}\,\mathrm{sign}(\omega)\right]\right\}} \\ \noalign{\vskip2pt}\hline\noalign{\vskip2pt} \dfrac{1}{\omega^2 - \omega_{\mathrm{P}}^2\left[1 + \mathrm{j}\eta_{\mathrm{P}}\,\mathrm{sign}(\omega)\right]} \end{bmatrix} \tag{21}$$

Numerical examples

The accuracy of the approximations summarized in the previous subsections has been investigated in the frequency domain. In Figure 5 the absolute value of the exact FRFs of both P and S substructures (solid lines) are compared with those given by LSS approximation (Eqs. (20), circles) and cascade approximation (Eqs. (21), dashed lines). The mass ratio and the tuning parameter are $\alpha = 0.02$ and $\beta = 1.0$, respectively, while the loss factors for the P and S substructures are $\eta_{\mathrm{S}} = 0.04$ and $\eta_{\mathrm{P}} = 0.10$. The comparisons demonstrate that the proposed LSS approximation is in good agreement with the exact solution even when the P and S oscillators are perfectly tuned, i.e. $\beta = 1.0$. On the contrary, the cascade approximation is unable to recover the bimodal FRF of the P oscillator (Fig. 5 left), and overestimates the peak for the S oscillator (Fig. 5 right). The semi-logarithmic plots in Figure 6 confirm the higher accuracy of the proposed LSS approximation (circles) with respect to the classical cascade approximation (dashed line) for a larger mass ratio ($\alpha = 0.10$) and different values of the tuning parameter ($\beta = 0.50$, 1.0 and 1.5). However, only when $\beta = 1.0$ the inaccuracy of the cascade approximation drastically affects the results.

APPROXIMATE RESPONSE OF MULTI-DOF COMBINED P-S SYSTEMS

Let us go back to the modal equations of motion of multi-DoF P and S substructures (Eqs. (7) and (8)). The comparison with the first of Eqs. (13) suggests that in the first of Eqs. (8) the out-of-diagonal term $\mathbf{m}_{\mathrm{SP}}$ in the modal matrix of inertia, $\mathbf{m}$, is proportional to the square root of the mass ratio, $\sqrt{\alpha}$ (not negligible), while the increment $\Delta\mathbf{m}_{\mathrm{P}}$ is proportional to the mass ratio, α (negligible). Accordingly, the inverse of the matrix $\mathbf{m}$ for multi-DoF P and S substructures can be approximated in a form similar to that one presented in Eq. (18) for single-DoF P and S oscillators:

$$\hat{\mathbf{m}}^{-1} \cong \left[\begin{array}{c|c} \mathbf{I}_{m_{\mathrm{S}}} + \mathbf{m}_{\mathrm{SP}}\,\mathbf{m}_{\mathrm{SP}}^{\mathrm{T}} & -\mathbf{m}_{\mathrm{SP}} \\ \hline -\mathbf{m}_{\mathrm{SP}}^{\mathrm{T}} & \mathbf{I}_{m_{\mathrm{P}}} \end{array} \right] \tag{22}$$

Following this approach, also the dynamic stiffness matrix and the influence vector take approximate forms similar to those derived in the case of single-DoF P and S oscillators (Eqs. (16)):

$$\hat{\mathbf{k}}(\omega) = \left[\begin{array}{c|c} \boldsymbol{\Omega}_{\mathrm{S}}^2 \, \gamma(\omega) & \mathbf{0} \\ \hline \mathbf{0} & \boldsymbol{\Omega}_{\mathrm{P}}^2 \end{array} \right] \times \left[1 + \mathrm{j} \eta_{\mathrm{P}} \, \mathrm{sign}(\omega) \right] \quad ; \quad \hat{\mathbf{g}} = - \left[\begin{array}{c} \mathbf{p}_{\mathrm{S}} \\ \mathbf{p}_{\mathrm{P}} \end{array} \right] \tag{23}$$

Then, substitution of Eqs. (22) and (23) into Eq. (11) gives expressions similar to those of Eqs. (17):

$$\hat{\mathbf{A}}(\omega) = \hat{\mathbf{m}}^{-1} \hat{\mathbf{k}}(\omega) = \left[\begin{array}{c|c} \left(\mathbf{I}_{m_{\mathrm{S}}} + \mathbf{m}_{\mathrm{SP}} \, \mathbf{m}_{\mathrm{SP}}^{\mathrm{T}} \right) \boldsymbol{\Omega}_{\mathrm{S}}^2 \, \gamma(\omega) & -\mathbf{m}_{\mathrm{SP}} \, \boldsymbol{\Omega}_{\mathrm{P}}^2 \\ \hline -\mathbf{m}_{\mathrm{SP}}^{\mathrm{T}} \boldsymbol{\Omega}_{\mathrm{S}}^2 \, \gamma(\omega) & \boldsymbol{\Omega}_{\mathrm{P}}^2 \end{array} \right] \times \left[1 + \mathrm{j} \eta_{\mathrm{P}} \, \mathrm{sign}(\omega) \right]$$

$$\hat{\mathbf{b}} = \hat{\mathbf{m}}^{-1} \hat{\mathbf{g}} = - \left[\begin{array}{c} \mathbf{p}_{\mathrm{S}} - \mathbf{m}_{\mathrm{SP}} \, \mathbf{p}_{\mathrm{P}} \\ \hline \mathbf{p}_{\mathrm{P}} \end{array} \right] \tag{24}$$

Moreover, substitution of Eqs. (24) into Eqs. (19) gives the array of the modal FRFs in the form:

$$\hat{\mathbf{h}}(\omega) = - \left\{ \left[\begin{array}{c|c} \hat{\mathbf{A}}_{\mathrm{S}} \, \gamma(\omega) & \hat{\mathbf{A}}_{\mathrm{SP}} \\ \hline \hat{\mathbf{A}}_{\mathrm{PS}} \, \gamma(\omega) & \boldsymbol{\Omega}_{\mathrm{P}}^2 \end{array} \right] \times \left[1 + \mathrm{j} \eta_{\mathrm{P}} \, \mathrm{sign}(\omega) \right] - \omega^2 \left[\begin{array}{c|c} \mathbf{I}_{m_{\mathrm{S}}} & \mathbf{0} \\ \hline \mathbf{0} & \mathbf{I}_{m_{\mathrm{P}}} \end{array} \right] \right\}^{-1} \cdot \left[\begin{array}{c} \hat{\mathbf{b}}_{\mathrm{S}} \\ \hline \mathbf{p}_{\mathrm{P}} \end{array} \right] \tag{25}$$

where $\hat{\mathbf{A}}_{\mathrm{S}} = \left(\mathbf{I}_{m_{\mathrm{S}}} + \mathbf{m}_{\mathrm{SP}} \, \mathbf{m}_{\mathrm{SP}}^{\mathrm{T}} \right) \boldsymbol{\Omega}_{\mathrm{S}}^2$, $\hat{\mathbf{A}}_{\mathrm{SP}} = -\mathbf{m}_{\mathrm{SP}} \, \boldsymbol{\Omega}_{\mathrm{P}}^2$, $\hat{\mathbf{A}}_{\mathrm{PS}} = -\mathbf{m}_{\mathrm{SP}}^{\mathrm{T}} \boldsymbol{\Omega}_{\mathrm{S}}^2$ and $\hat{\mathbf{b}}_{\mathrm{S}} = \mathbf{p}_{\mathrm{S}} - \mathbf{m}_{\mathrm{SP}} \, \mathbf{p}_{\mathrm{P}}$. Interestingly, in Eq. (25) only the direct terms of the P substructure, namely the squared spectral matrix, $\boldsymbol{\Omega}_{\mathrm{P}}^2$, and the array of the modal participating factors, $\mathbf{p}_{\mathrm{P}}$, are unmodified by the coupling matrix $\mathbf{m}_{\mathrm{SP}}$. Finally, once the array of Eq. (25) is partitioned as $\hat{\mathbf{h}}(\omega) = \left[\hat{\mathbf{h}}_{\mathrm{S}}^{\mathrm{T}}(\omega) \mid \hat{\mathbf{h}}_{\mathrm{P}}^{\mathrm{T}}(\omega) \right]^{\mathrm{T}}$, that one of the DoFs can be written similarly to Eq. (20):

$$\hat{\mathbf{H}}(\omega) = \boldsymbol{\Gamma} \hat{\mathbf{h}}(\omega) = \left[\begin{array}{c} \boldsymbol{\Phi}_{\mathrm{S}} \, \hat{\mathbf{h}}_{\mathrm{S}}(\omega) + \boldsymbol{\Psi}_{\mathrm{SP}} \, \hat{\mathbf{h}}_{\mathrm{P}}(\omega) \\ \hline \boldsymbol{\Phi}_{\mathrm{P}} \, \hat{\mathbf{h}}_{\mathrm{P}}(\omega) \end{array} \right]$$

MAXIMUM SECONDARY RESPONSE BY EARTHQUAKE RESPONSE SPECTRUM

Aim of this section is to derive a novel definition of the cross-correlation coefficients $\rho(i,k)$ that enables the Complete Quadratic Combination (CQC) rule (Wilson et al., 1981) to be extended to the seismic analysis and design of multi-DoF Secondary (S) substructures attached to a multi-DoF Primary (P) load-bearing substructure. It is worth noting that, in order to be attractive for practical applications: i) the proposed combination rule takes advantage of the LSS (Ligh Secondary Substructure) approximation presented in the previous sections, and operates without evaluating the eigenproperties of the combined P-S system; while ii) the seismic input is represented through a conventional earthquake response spectrum. Following the same idea underlying earlier papers by Falsone and Muscolino (1999 and 2004), in fact, the proposed cross-correlation coefficients incorporate the dynamic effects which complicate the seismic response of S substructures with respect to conventional base-fixed structures with equal viscous damping ratio in all the modes of vibration.

Preliminary expressions

Let $y_S(t)$ be a generic response of interest (e.g., an internal force or a deformation measure) for the S attachment as well as for the P-S anchors. Owing to the linearity of both P and S substructures, $y_S(t)$ can be expressed as linear combination of the modal coordinates of the coupled P-S system:

$$y_S(t) = \mathbf{E}_{SS}^T \mathbf{u}_S(t) + \mathbf{E}_{SP}^T \mathbf{u}_P(t) = \mathbf{E}_{SS}^T \boldsymbol{\Phi}_S \mathbf{q}_S(t) + \left(\mathbf{E}_{SS}^T \boldsymbol{\Psi}_{SP} + \mathbf{E}_{SP}^T \boldsymbol{\Phi}_P \right) \mathbf{q}_P(t)$$

$$= \mathbf{e}_{SS}^T \mathbf{q}_S(t) + \mathbf{e}_{SP}^T \mathbf{q}_P(t) = \sum_{i=1}^{m_S} e_{SSi} \, q_{Si}(t) + \sum_{i=1}^{m_P} e_{SPi} \, q_{Pi}(t)$$

where $\mathbf{E}_{SS}$ (of dimensions $n_S \times 1$) and $\mathbf{E}_{SP}$ ($n_P \times 1$) are the arrays listing the contributing coefficients for the DoFs, while the corresponding ones for the modal coordinates are given by $\mathbf{e}_{SS} = \boldsymbol{\Phi}_S^T \mathbf{E}_S$ (of dimensions $m_S \times 1$) and $\mathbf{e}_{SP} = \boldsymbol{\Phi}_P^T \mathbf{E}_{SP} + \boldsymbol{\Psi}_{SP}^T \mathbf{E}_{SS}$ ($m_P \times 1$). According to the CQC rule (Wilson et al., 1981), the maximum seismic response can be computed as:

$$\max|y_{\mathrm{S}}(t)| = \Bigg[\sum_{i=1}^{m_{\mathrm{S}}} \sum_{k=1}^{m_{\mathrm{S}}} \rho_{\mathrm{SS}}(i,k)\, e_{\mathrm{SS}i}\, e_{\mathrm{SS}k} \max|q_{\mathrm{S}i}(t)| \max|q_{\mathrm{S}k}(t)|$$
$$+ \sum_{i=1}^{m_{\mathrm{P}}} \sum_{k=1}^{m_{\mathrm{P}}} \rho_{\mathrm{PP}}(i,k)\, e_{\mathrm{SP}i}\, e_{\mathrm{SP}k} \max|q_{\mathrm{P}i}(t)| \max|q_{\mathrm{P}k}(t)| \qquad (26)$$
$$+ 2 \sum_{i=1}^{m_{\mathrm{S}}} \sum_{k=1}^{m_{\mathrm{P}}} \rho_{\mathrm{SP}}(i,k)\, e_{\mathrm{SS}i}\, e_{\mathrm{SP}k} \max|q_{\mathrm{S}i}(t)| \max|q_{\mathrm{P}k}(t)| \Bigg]^{1/2}$$

where the symbol $\rho_{\mathrm{AB}}(i,k)$ stands for the cross-correlation coefficient among the i-th modal coordinate of the A substructure, $q_{\mathrm{A}i}(t)$, and the k-th modal coordinate of the B substructure, $q_{\mathrm{B}k}(t)$, being $\mathrm{A} = \mathrm{P},\mathrm{S}$ and $\mathrm{B} = \mathrm{P},\mathrm{S}$, $i = 1,\cdots,m_{\mathrm{A}}$ and $k = 1,\cdots,m_{\mathrm{B}}$:

$$\rho_{\mathrm{AB}}(i,k) = \frac{\mathrm{E}\langle q_{\mathrm{A}i}(t)\, q_{\mathrm{B}k}(t) \rangle}{\sqrt{\mathrm{E}\langle q_{\mathrm{A}i}^2(t) \rangle \mathrm{E}\langle q_{\mathrm{B}k}^2(t) \rangle}} \qquad (27)$$

in which the symbol $\mathrm{E}\langle \cdot \rangle$ denotes the expectation operator. These coefficients are usually evaluated under the assumption that the seismic acceleration is a zero-mean stationary Gaussian process, which can be modelled as white noise (Der Kiureghian, 1981), filtered white noise (Der Kiureghian and Nakamura, 1993) or spectrum-compatible coloured process (Cacciola et al., 2004). Moreover, it should be emphasized that the CQC rule has been originally derived under the assumption that the Peak Factor, PF, of the structural response of interest, $y(t)$, is approximately equal to the peak factors of the contributing modal coordinates, $q_i(t)$, that is:

$$PF = \frac{\max|y(t)|}{\sqrt{\mathrm{E}\langle y^2(t) \rangle}} = \frac{\max|q_i(t)|}{\sqrt{\mathrm{E}\langle q_i^2(t) \rangle}} \qquad (28)$$

Proposed cross-correlation coefficients

Let us now rewrite Eq. (27) in the equivalent form:

$$\rho_{\mathrm{AB}}(i,k) = r_{\mathrm{AB}}(i,k) \frac{\hat{b}_{\mathrm{A}i}\, \hat{b}_{\mathrm{B}k}\, \sigma_{\mathrm{A}i}\, \sigma_{\mathrm{B}k}}{\sqrt{\mathrm{E}\langle q_{\mathrm{A}i}^2(t) \rangle} \sqrt{\mathrm{E}\langle q_{\mathrm{B}k}^2(t) \rangle}} \qquad (29)$$

where:

$$r_{\mathrm{AB}}(i,k) = \frac{\mathrm{E}\langle q_{\mathrm{A}i}(t)\, q_{\mathrm{B}k}(t) \rangle}{\left(\hat{b}_{\mathrm{A}i}\, \sigma_{\mathrm{A}i}\right)\left(\hat{b}_{\mathrm{B}k}\, \sigma_{\mathrm{B}k}\right)} \qquad (30)$$

15

σ_{Ai} and σ_{Bk} being the standard deviations of the stationary seismic response of auxiliary single-DoF oscillators having unitary mass, a reference value of the viscous damping ratio, ζ_{ref}, for which the earthquake response spectrum is known (usually, $\zeta_{ref} = 0.05$), and undamped natural periods given by the corresponding ones of the decoupled substructures; for instance, the undamped natural period of the Ai -th auxiliary oscillator is:

$$T_{Ai} = \frac{2\pi}{\omega_{Ai}} \quad (A = P, S ; i = 1, \cdots, m_A)$$

According to the second of Eqs. (24), moreover, the coefficient $\hat{b}_{Ai}$ in Eqs. (29) and (30), which play the role of modal participating factors, takes different expressions for P and S substructures:

$$\hat{b}_{Ai} = \begin{cases} -p_{Pi} , & A = P \\ -p_{Si} + \boldsymbol{\phi}_{Si}^T \sum_{k=1}^{m_P} p_{Pk} \, \mathbf{M}_S \, \boldsymbol{\psi}_{SPk} , & A = S \end{cases}$$

That is, for the P substructure the coefficients $\hat{b}_{Pi}$ are the modal participating factors p_{Pi} evaluated without considering the presence of attachments (second of Eqs. (9)), while for the S substructure the coefficients $\hat{b}_{Si}$ are given by the modal participating factors p_{Si} of the base-fixed attachment (first of Eqs. (9)) appropriately modified by the interaction with the P structural system.

As a result of the above definitions, the product $\left(\hat{b}_{Ai} \, \sigma_{Ai} \right)$ in Eq. (30) is the standard deviation of the steady-state response of a classical single-DoF oscillator ruled by:

$$\ddot{q}_{Ai}^{(0)}(t) + 2 \zeta_{ref} \, \omega_{Ai} \, \dot{q}_{Ai}^{(0)}(t) + \omega_{Ai}^2 \, q_{Ai}^{(0)}(t) = \hat{b}_{Ai} \, \ddot{u}_g(t)$$

Under the assumption that the ground acceleration is a white noise of unitary one-sided power spectral density, this quantity is known in closed-form:

$$\left(\hat{b}_{Ai} \, \sigma_{Ai} \right) = \sqrt{E \left\langle \left[q_{Ai}^{(0)}(t) \right]^2 \right\rangle} = \frac{1}{2} \sqrt{\frac{\pi}{\zeta_{ref} \, \omega_{Ai}^3}} \tag{31}$$

On the other hand, the expectation in the numerator of Eq. (30) can be evaluated in the frequency domain through the numerical integral:

$$\mathrm{E}\left\langle q_{\mathrm{A}i}(t)\, q_{\mathrm{B}k}(t)\right\rangle = \int\limits_{0}^{\omega_{\mathrm{c}}} \hat{h}_{\mathrm{A}i}(\omega)\, \hat{h}_{\mathrm{B}k}^{*}(\omega)\, \mathrm{d}\omega \tag{32}$$

where ω_{c} is the cut-off circular frequency, the superscripted asterisk means complex conjugate, and where $\hat{h}_{\mathrm{A}i}(\omega)$ and $\hat{h}_{\mathrm{B}k}(\omega)$ are the approximate complex-valued FRFs of the modal coordinates $q_{\mathrm{A}i}(t)$ and $q_{\mathrm{B}k}(t)$, given by the i-th element of $\hat{\mathbf{h}}_{\mathrm{A}}(\omega)$ and the k-th element of $\hat{\mathbf{h}}_{\mathrm{B}}(\omega)$, respectively. It is worth noting that, although effective in a number of real circumstances, the assumption of white noise input should be carefully checked in the cases of soft soil and/or stiff structural system (Der Kiureghian and Nakamura, 1993; Cacciola et al., 2004; Palmeri, 2006). Since the proposed cross-correlation coefficients are evaluated in the frequency domain, however, the effects of a non-white input can be easily included.

Eqs. (31) and (32), thus, allow evaluating the new coefficients $r_{\mathrm{AB}}(i,k)$ defined in Eq. (30), which in turn allow to rewrite each term in the double summations of Eqs. (26) as:

$$\rho_{\mathrm{AB}}(i,k)\max\left|q_{\mathrm{A}i}(t)\right|\max\left|q_{\mathrm{B}k}(t)\right| = r_{\mathrm{AB}}(i,k)\left[\frac{\hat{b}_{\mathrm{A}i}\,\sigma_{\mathrm{A}i}\max\left|q_{\mathrm{A}i}(t)\right|}{\sqrt{\mathrm{E}\left\langle q_{\mathrm{A}i}^{2}(t)\right\rangle}}\right]\left[\frac{\hat{b}_{\mathrm{B}k}\,\sigma_{\mathrm{B}k}\max\left|q_{\mathrm{B}k}(t)\right|}{\sqrt{\mathrm{E}\left\langle q_{\mathrm{B}k}^{2}(t)\right\rangle}}\right]$$

Taking into account Eq. (28), the latter expression can be approximated as:

$$\rho_{\mathrm{AB}}(i,k)\max\left|q_{\mathrm{A}i}(t)\right|\max\left|q_{\mathrm{B}k}(t)\right| = r_{\mathrm{AB}}(i,k)\hat{b}_{\mathrm{A}i}\,\hat{b}_{\mathrm{B}k}\left[\sigma_{\mathrm{A}i}\cdot PF\right]\left[\sigma_{\mathrm{B}k}\cdot PF\right]$$

Moreover, the terms $\left[\sigma_{\mathrm{A}i}\cdot PF\right]$ and $\left[\sigma_{\mathrm{B}k}\cdot PF\right]$ can be viewed as the maximum seismic responses of the auxiliary single-DoF oscillators with undamped natural periods $T_{\mathrm{A}i}$ and $T_{\mathrm{B}k}$, respectively, and so the previous expression can be rewritten as:

$$\rho_{\mathrm{AB}}(i,k)\max\left|q_{\mathrm{A}i}(t)\right|\max\left|q_{\mathrm{B}k}(t)\right| = r_{\mathrm{AB}}(i,k)\hat{b}_{\mathrm{A}i}\,\hat{b}_{\mathrm{B}k}\frac{S_{\mathrm{a}}\left(T_{\mathrm{A}i},\zeta_{\mathrm{ref}}\right)}{\left(2\pi/T_{\mathrm{A}i}\right)^{2}}\frac{S_{\mathrm{a}}\left(T_{\mathrm{B}k},\zeta_{\mathrm{ref}}\right)}{\left(2\pi/T_{\mathrm{B}k}\right)^{2}} \tag{33}$$

where $S_{\mathrm{a}}\left(T,\zeta\right)$ denotes the earthquake response spectrum in terms of pseudo-acceleration for undamped natural period T and viscous damping ratio ζ, and where the coefficients $r_{\mathrm{AB}}(i,k)$ are given by substituting Eq. (31) into Eq. (30):

$$r_{\mathrm{AB}}(i,k) = \frac{4\zeta_{\mathrm{ref}}}{\pi}\omega_{\mathrm{A}i}\,\omega_{\mathrm{B}k}\,\sqrt{\omega_{\mathrm{A}i}\,\omega_{\mathrm{B}k}}\,\mathrm{E}\left\langle q_{\mathrm{A}i}(t)\, q_{\mathrm{B}k}(t)\right\rangle$$

in which only the expectation of Eq. (32) has to be computed. Finally, upon substitution of Eq. (33) into Eq. (26), one obtains the CQC rule for the response of interest:

$$
\begin{aligned}
\max\left|y_{\mathrm{S}}(t)\right| = \frac{1}{4\pi^2}\Bigg[& \sum_{i=1}^{m_{\mathrm{S}}}\sum_{k=1}^{m_{\mathrm{S}}} r_{\mathrm{SS}}(i,k)\, e_{\mathrm{SS}i}\, e_{\mathrm{SS}k}\, \hat{b}_{\mathrm{S}i}\, \hat{b}_{\mathrm{S}k}\, T_{\mathrm{S}i}^2\, T_{\mathrm{S}k}^2\, S_{\mathrm{a}}\left(T_{\mathrm{S}i},\zeta_{\mathrm{ref}}\right) S_{\mathrm{a}}\left(T_{\mathrm{S}k},\zeta_{\mathrm{ref}}\right) \\
& + \sum_{i=1}^{m_{\mathrm{P}}}\sum_{k=1}^{m_{\mathrm{P}}} r_{\mathrm{PP}}(i,k)\, e_{\mathrm{SP}i}\, e_{\mathrm{SP}k}\, \hat{b}_{\mathrm{P}i}\, \hat{b}_{\mathrm{P}k}\, T_{\mathrm{P}i}^2\, T_{\mathrm{P}k}^2\, S_{\mathrm{a}}\left(T_{\mathrm{P}i},\zeta_{\mathrm{ref}}\right) S_{\mathrm{a}}\left(T_{\mathrm{P}k},\zeta_{\mathrm{ref}}\right) \\
& + 2\sum_{i=1}^{m_{\mathrm{S}}}\sum_{k=1}^{m_{\mathrm{P}}} r_{\mathrm{SP}}(i,k)\, e_{\mathrm{SS}i}\, e_{\mathrm{SP}k}\, \hat{b}_{\mathrm{S}i}\, \hat{b}_{\mathrm{P}k}\, T_{\mathrm{S}i}^2\, T_{\mathrm{P}k}^2\, S_{\mathrm{a}}\left(T_{\mathrm{S}i},\zeta_{\mathrm{ref}}\right) S_{\mathrm{a}}\left(T_{\mathrm{P}k},\zeta_{\mathrm{ref}}\right)\Bigg]^{1/2}
\end{aligned}
\tag{34}
$$

NUMERICAL APPLICATION

The CQC rule proposed in the previous section has been applied to the 6-DoF P-S system shown in Figure 7. The P substructure is a planar shear-type 3-DoF frame, with storey mass $M_{\mathrm{P}} = 3{,}000\,\mathrm{kg}$ and storey stiffness $K_{\mathrm{P}} = 3{,}000\,\mathrm{kN/m}$, while the loss coefficient is $\eta_{\mathrm{P}} = 0.10$ (the equivalent viscous damping ratio is $\zeta_{\mathrm{P}} = \eta_{\mathrm{P}}/2 = 0.05$). The S substructure is a 3-DoF attachment, with lumped mass $M_{\mathrm{S}} = \alpha\, M_{\mathrm{P}}$, lumped stiffness $K_{\mathrm{S}} = 889\,\alpha\,\beta^2\,\mathrm{kN/m}$ and anchor stiffness $K_{\mathrm{SP}} = 1{,}207\,\alpha\,\beta^2\,\mathrm{kN/m}$ (the dimensionless variables α and β being the mass ratio and a tuning parameter, respectively), while the loss coefficient is $\eta_{\mathrm{S}} = 0.04$ (equivalent viscous damping ratio $\zeta_{\mathrm{S}} = 0.02$). The undamped modal circular frequencies of the base-fixed substructures, solutions of the eigenproblems given in Eqs. (6), are $\omega_{\mathrm{P1}} = 16.4$, $\omega_{\mathrm{P2}} = 44.7$ and $\omega_{\mathrm{P3}} = 61.1\,\mathrm{rad/s}$ for the P frame, and $\omega_{\mathrm{S1}} = 16.4\,\beta$, $\omega_{\mathrm{S2}} = 28.6\,\beta$ and $\omega_{\mathrm{S3}} = 34.6\,\beta\,\mathrm{rad/s}$ for the S attachment.

When the coupled P-S system is considered, the undamped modal circular frequencies, ω_i, and the corresponding viscous damping ratios, ζ_i (with $i = 1, \cdots, 6$), strongly depends on mass ratio and tuning parameter. For the aim of comparison, the values of ω_i (in $\mathrm{rad/s}$) and of ζ_i (dimensionless), given by the Modal Strain Energy (Johnson and Kienholz, 1982), are listed in Table 1 for $\alpha = 0.05$ and $\beta = 0.50$, 1.00 and 1.50. Interestingly, all the computed viscous damping ratios are in the range $0.02 \le \zeta_i \le 0.05$, and take values close to $\zeta_{\mathrm{P}} = 0.05$ or to $\zeta_{\mathrm{S}} = 0.02$ when the corresponding modal shapes resembles those of the P frame or of the S attachment, respectively; on the contrary, intermediate values of the viscous damping ratio indicate coupling between the base-fixed modal shapes of P and S substructures (e.g., ω_1 and ω_2 for $\beta = 1.00$; ω_3 and ω_4 for $\beta = 1.50$).

18

The reference earthquake response spectrum for the viscous damping ratio $\zeta_{ref} = 0.05$ (Fig. 8, thick line) has been defined by averaging those of eight recorded accelerograms (Fig. 8, thin lines) normalized with respect to the Peak Ground Acceleration (*PGA*); these accelerograms, depicted in Figure 9, are the orthogonal components of the four strong ground motions chronologically listed in Table 2 (PEER, 2000).

The average drifts in the S attachment, i.e. the mean value of the strains in the secondary springs k_S (Fig. 7), and the average deformations in the P-S anchors, i.e. the mean value of the strains in the Primary-Secondary springs k_{SP} (Fig. 7), have been selected as seismic responses of interest. Two values of the mass ratio, $\alpha = 0.01$ and 0.05, has been considered. Only the first mode has been retained for the P frame ($m_P = 1$, modal participating mass= 92.3%) in the proposed CQC rule (Eq. (34)), while two modes have been retained for the S attachment ($m_S = 2$, modal participating mass= 89.5%). Figure 10 shows the percentage error ε as function of the tuning parameter in the range $0.5 \leq \beta \leq 2.0$, assuming that the "exact" values are the respective average maxima given by the eight time history analyses. The accuracy of the proposed approach (solid line) proves to be very good from an engineering point of view: more precisely, in the case of "soft" attachments ($0.5 \leq \beta \leq 1.2$) the results are slightly conservative ($0 < \varepsilon < 25\%$), while for "stiff" attachments ($1.2 \leq \beta \leq 2.0$) the seismic demand is slightly underestimated ($-25 < \varepsilon < 0\%$). A couple of considerations would confirm the effectiveness of the proposed method: i) the numerical test is extremely severe, since the analyses are carried out not with stochastically generated accelerograms, but with recorded accelerograms, having quite different time-frequency properties; and ii) the level of confidence is similar to that one of the original CQC rule for classically damped structures. On the contrary, a conventional analysis with the earthquake response spectrum based on the cascade approximation (dashed lines) proves to be absolutely inadequate: the seismic response of soft attachments, in fact, is heavily underestimated, since the percentage error may be as low as -100%; conversely, the results for the anchors of stiff attachment are excessively conservative, since the percentage error may be larger than 100%. It is worth noting that, according to the current Italian seismic code (Presidenza del Consiglio dei Ministri, 2003), in our analyses the conventional response of the S attachment has been

evaluated as the quasi-static response to the seismic motion of the P frame. More precisely, in this cascade approximation the maximum seismic response, $\max|y_S(t)|$, is still given by Eq. (26) in which, however, the coefficients $\rho_{SS}(i,k)$ and $\rho_{SP}(i,k)$ go to zero and in which $\rho_{PP}(i,k)$ are the cross-correlation coefficients proposed by Der Kiureghian (1981).

CONCLUSIONS

In this paper, a novel Complete Quadratic Combination (CQC) rule for the seismic analysis and design of multi-DoF Secondary (S) attachments to multi-DoF Primary (P) structural systems has been proposed and numerically validated. In a first stage, in contrast with the classical "cascade" approximation, which neglects the feedback of the S substructure on the P one, the accuracy of a "Light Secondary Substructure" (LSS) approximation has been proved. In a second stage, the latter approximation has been used in evaluating the cross-correlation coefficients in the CQC rule. These coefficients are quite different from those available in the literature, since they would directly include in the combination rule the effects of frequency tuning among P and S frequencies and different damping ratios in the components. For the validation purposes, the results of a severe numerical investigation, with eight recorded accelerograms, are presented and discussed.

Two main features could make the proposed method particularly attractive for practical analyses: i) modal frequencies and modal shapes used in the combination rule are those of the decoupled substructures, assumed to be fixed to their own bases, i.e. the eigenproperties of the combined P-S system are nor required; and ii) the earthquake response spectrum for only a single value of the viscous damping ratio is used, and this reference value can be different from the viscous damping ratios of the components.

Finally, it is worth noting that the cross-correlation coefficients have been derived in this paper under the restrictive assumptions that: i) the ground acceleration is a stationary white noise; ii) the peak factors of the structural response of interest are equal to those of the contributing modal coordinates. More accurate results, therefore, can be obtained by removing these assumptions, even if at the same time the procedure could become burdensome: these possible improvements will be the subject of future work.

REFERENCES

1. Amini, A. and Trifunac, M.D. (1985) "Statistical extension of response spectrum superposition," International Journal of Soil Dynamics and Earthquake Engineering, Vol. 4, No. 2, pp. 54-63.

2. Biot, M.A. (1932). "Vibrations of buildings during earthquake," Chapter II in Ph.D. Thesis No. 259, entitled "Transient Oscillations in Elastic System," Aeronautics Department, California Institute of Technology.

3. Biot, M.A. (1933). "Theory of elastic systems vibrating under transient impulse with an application to earthquake-proof buildings," Proceeding of the National Academy of Sciences, Vol. 19, No. 2, pp. 262–8.

4. Biot, M.A. (1934). "Theory of vibration of buildings during earthquakes," Zeitschrift für. Angewandte Matematik und Mechanik, Vol. 14, No. 4, pp. 213–23.

5. Cacciola, P., Colajanni, P. and Muscolino, G. (2004). "Combination of modal responses consistent with seismic input representation," ASCE Journal of Structural Engineering, Vol. 130, No. 1, pp. 47-55.

6. Chen, Y. and Soong, T.T. (1988). "State-of-the-art review: seismic response of secondary systems," Engineering Structures, Vol. 10, No. 4, pp. 218-28.

7. Dey, A. and Gupta, V.K. (1999). "Stochastic seismic response of multiply-supported secondary systems in flexible-base structures," Earthquake Engineering and Structural Dynamics, Vol. 28, No. 4, pp. 351-69.

8. Der Kiureghian, A. (1981). "A response spectrum method for random vibration analysis of MDF stystems," Earthquake Engineering and Structural Dynamics, Vol. 9, No. 5, pp. 419-35.

9. Der Kiureghian, A. and Nakamura, Y. (1993). "CQC modal combination rule for high-frequency modes," Earthquake Engineering and Structural Dynamics, Vol. 22, No. 11, pp. 943-56.

10. Der Kiureghian, A. and Neuenhofer, A. (1992). "Response spectrum method for multi-support seismic excitations," Earthquake Engineering and Structural Dynamics, Vol. 21, No. 8, pp. 713-40.

11. Falsone, G. and Muscolino, G. (1999). "Cross-correlation coefficients and modal combination rules for non-classically damped systems," Earthquake Engineering and Structural Dynamics, Vol. 28, No. 22, pp. 1669-84.

12. Falsone, G. and Muscolino, G. (2004). "New real-value modal combination rules for non-classically damped structures," Earthquake Engineering and Structural Dynamics, Vol. 33, No. 12, pp. 1187-209.

13. Falsone, G., Muscolino, G., and Ricciardi, G. (1991). "Combined dynamic response of primary and multiply connected cascaded secondary subsystems," Earthquake Engineering and Structural Dynamics, Vol. 20, No. 8, pp. 749-67.

14. Feriani, A. and Perotti, F. (1996). "The formation of viscous damping matrices for the dynamic analysis of MDOF systems," Earthquake Engineering and Structural Dynamics, Vol. 25 No. 7, pp. 689-709.

15. Gupta, A.K. and Jaw, J.W. (1986). "Seismic response of nonclassically damped systems," Nuclear Engineering and Design, Vol. 91, No. 2, pp. 153-9.

16. Gupta, I.D. and Trifunac, M.D. (1988). "Order statistics of peaks in earthquake response," ASCE Journal of Engineering Mechanics, Vol. 114, No. 10, pp. 1605-27.

17. Gupta V.K. and Trifunac, M.D. (1989). "Investigation of building response to translational and rotational earthquake excitations," Report No. 89-02, Department of Civil Engineering, University of Southern California.

18. Inaudi, J.A. and Kelly, J.M. (1995). "Linear hysteretic damping and the Hilbert transform," ASCE Journal of Engineering Mechanics, Vol. 121, No. 5, pp. 626-32.

19. Iwan, W.D. (1997) "Drift spectrum: Measure of demand for earthquake ground motions," ASCE Journal of Structural Engineering, Vol. 123, No. 4, pp. 397-404.

20. Johnson, C.D. and Kienholz, D.A. (1982). "Finite element prediction of damping in structures with constrained viscoelastic layers," AIAA Journal, Vol. 20 No. 9, pp. 1284-90.

21. Lavelle, F.M., Bergman, L.A. and Spanos, P.D. (1991). "Seismic response spectra of a combined system by Green's functions," Soil Dynamics and Earthquake Engineering, Vol. 10, No. 2, pp. 93-100.

22. Makris, N. (1997). "Causal hysteretic element," ASCE Journal of Engineering Mechanics, Vol. 123, No. 11, pp. 1209-14.

23. Makris, N. and Zhang, J. (2000). "Time domain viscoelastic analysis of earth structures," Earthquake Engineering and Structural Dynamics, Vol. 29, No. 6, pp. 745-68.

24. Muscolino, G. (1990). "Dynamic response of multiply connected primary-secondary systems," Earthquake Engineering and Structural Dynamics, Vol. 19, No. 2, pp. 205-16.

25. Muscolino, G., Palmeri, A. and Ricciardelli F. (2005). "Time-domain response of linear hysteretic systems to deterministic and random excitations," Earthquake Engineering and Structural Dynamics, Vol. 34, No. 9, pp. 1129-47.

26. Nashif, A.D., Jones, D.I. and Henderson, J.P. (1985). "Vibration Damping," John Wiley & Sons, New York.

27. Palmeri, A. (2006). "Correlation coefficients for structures with viscoelastic dampers," Engineering Structures, Vol. 28, No. 8, pp. 1197-208.

28. PEER, Pacific Earthquake Engineering Research Center (2000). "Strong Motion Database," <http://peer.berkeley.edu/smcat/>.

29. Presidenza del Consiglio dei Ministri (2003). "Ordinanza 3274: Primi elementi in materia di criteri generali per la classificazione sismica del territorio nazionale e di normative tecniche per le costruzioni in zona sismica," in Italian.

30. Singh, M.P. (1988). "Seismic design of secondary systems," Probabilistic Engineering Mechanics, Vol. 3, No. 3, pp. 151-8.

31. Singh, M.P., Moreschi, L.M., Suárez, L.E. and Matheu, E.E. (2006a). "Seismic design forces. I: Rigid nonstructural components," ASCE Journal of Structural Engineering, Vol. 132, No. 10, pp. 1524-32.

32. Singh, M.P., Moreschi, L.M., Suárez, L.E. and Matheu, E.E. (2006b). "Seismic design forces. I: Flexible nonstructural components," ASCE Journal of Structural Engineering, Vol. 132, No. 10, pp. 1533-42.

33. Villaverde, R. (2004). "Seismic analysis and design of nonstructural elements," In: Bozorgnia, Y. and Bertero, V.V. (Editors), "Earthquake Engineering from Engineering Seismology to Performance-Based Engineering," CRC Press, Boca Raton, Ch. 19.

34. Wilson, E.L., Der Kiureghian, A. and Bayo, E.P. (1981). "Replacement for the SRSS method in seismic analysis," Earthquake Engineering and Structural Dynamics, Vol. 9, No. 2, pp. 187-92.

LIST OF TABLES

LIST OF FIGURES

TABLE 1

$\alpha = 0.05,\ \beta = 0.50$		$\alpha = 0.05,\ \beta = 1.00$		$\alpha = 0.05,\ \beta = 1.50$	
$\omega_1 = 8.13$	$\zeta_1 = 0.0205$	$\omega_1 = 14.9$	$\zeta_1 = 0.0359$	$\omega_1 = 16.0$	$\zeta_1 = 0.0480$
$\omega_2 = 14.3$	$\zeta_2 = 0.0208$	$\omega_2 = 18.0$	$\zeta_2 = 0.0338$	$\omega_2 = 25.2$	$\zeta_2 = 0.0216$
$\omega_3 = 16.4$	$\zeta_3 = 0.0449$	$\omega_3 = 28.5$	$\zeta_3 = 0.0205$	$\omega_3 = 41.3$	$\zeta_3 = 0.0300$
$\omega_4 = 17.5$	$\zeta_4 = 0.0239$	$\omega_4 = 34.6$	$\zeta_4 = 0.0201$	$\omega_4 = 46.8$	$\zeta_4 = 0.0393$
$\omega_5 = 44.8$	$\zeta_5 = 0.0499$	$\omega_5 = 45.1$	$\zeta_5 = 0.0492$	$\omega_5 = 52.0$	$\zeta_5 = 0.0208$
$\omega_6 = 61.1$	$\zeta_6 = 0.0500$	$\omega_6 = 61.2$	$\zeta_6 = 0.0498$	$\omega_6 = 61.6$	$\zeta_6 = 0.0491$

Undamped natural frequencies (in rad/s) and viscous damping ratios (dimensionless) of the combined P-S system depicted in Figure 7 for mass ratio $\alpha = 0.05$ and tuning parameter $\beta = 0.50$, 1.00 and 1.50.

TABLE 2

Earthquake (Date)	M (Ml)	Station	Component	PGA [g]	PGV [cm/s]	PGD [cm]
Friuli, Italy (06-May-1976)	6.5 (6.2)	Tolmezzo	000	0.351	22.0	4.1
			270	0.315	30.8	5.1
Tabas, Iran (16-Sep-1978)	7.4 (7.7)	Tabas	LN	0.836	97.8	36.92
			TR	0.852	121.4	94.58
Irpinia, Italy (23-Nov-1980)	(6.5)	Sturno	000	0.251	37.0	11.77
			270	0.358	52.7	33.08
Kobe, Japan (16-Jan-1995)	6.9	Kakogawa	000	0.251	18.7	5.83
			090	0.345	27.6	9.6

Information pertinent to the strong motions selected in this study.

FIGURE 1
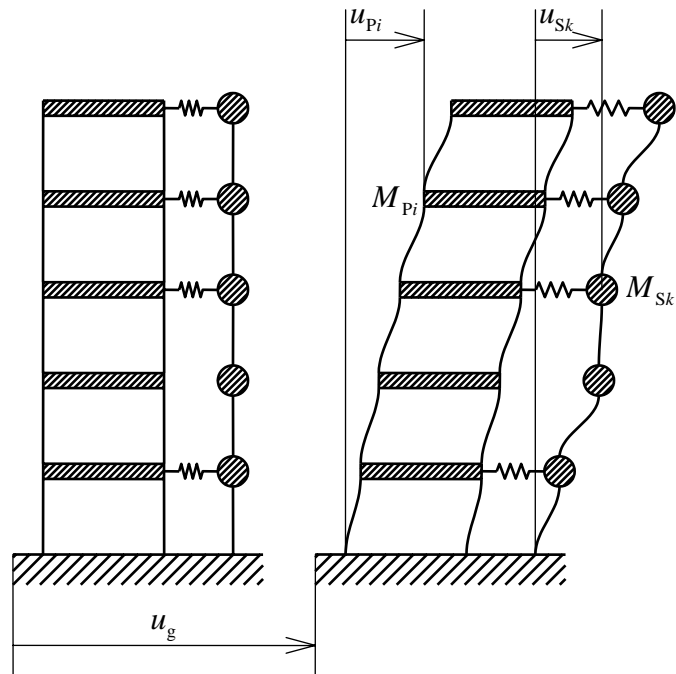
Sketch of combined Primary-Secondary (P-S) system.

FIGURE 2

a)   b)
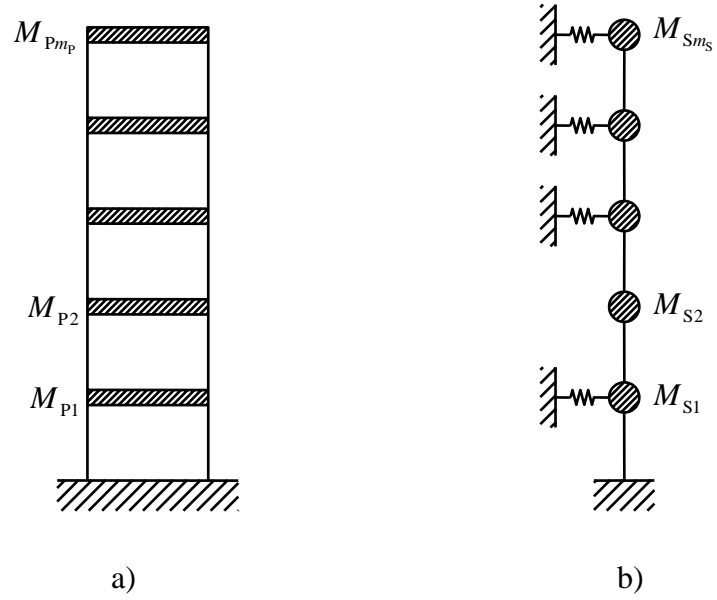
Base-fixed substructures: P structural system (a); S attachment (b).

FIGURE 3

a)   b)   c)
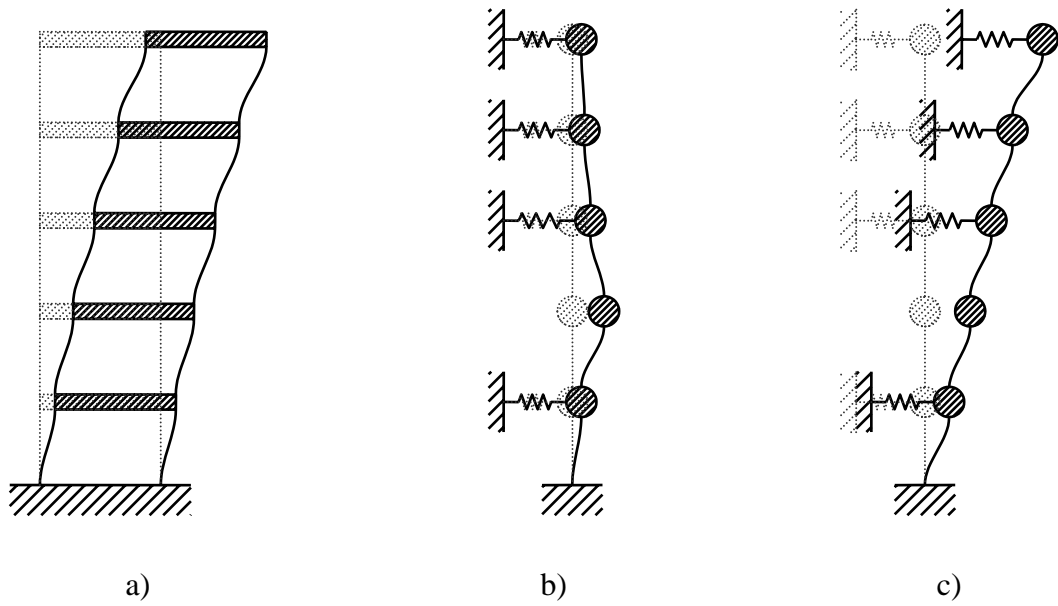
Modal shapes of the P structural system (a) and of the base-fixed S attachment (b); deformed shape of the S attachment induced by the modal shape of the P structural system (c).
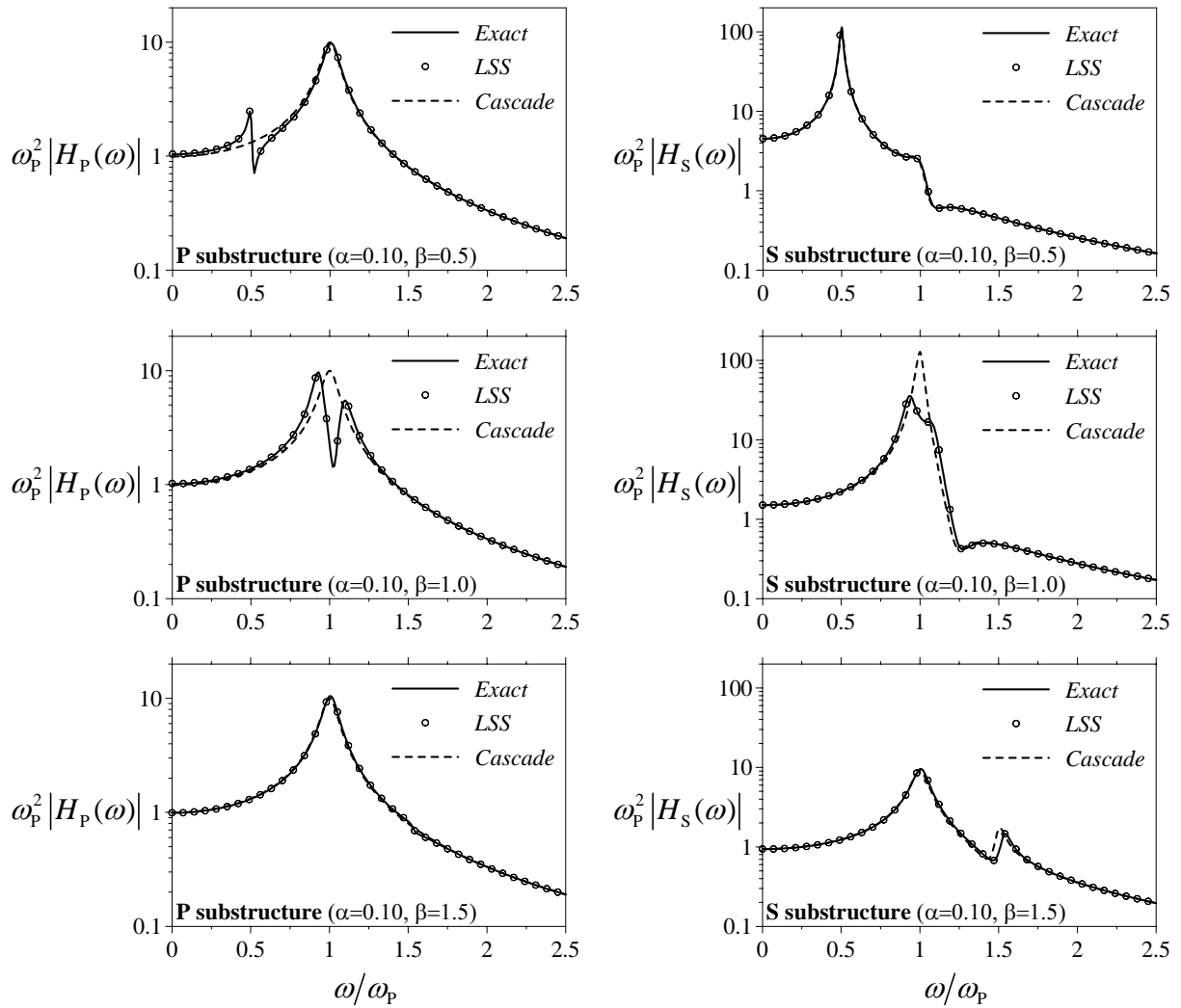
FIGURE 4
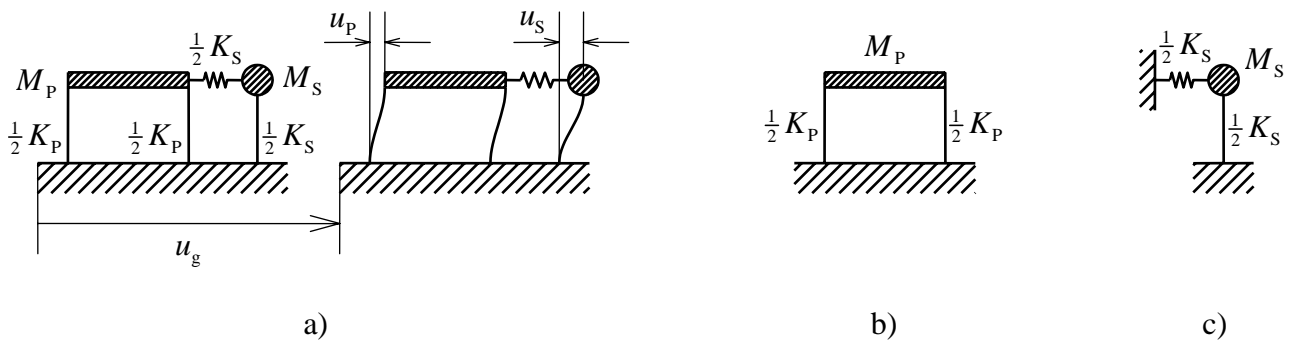

2-DoF combined P-S system (a); P oscillator (b); S oscillator (c).

FIGURE 5
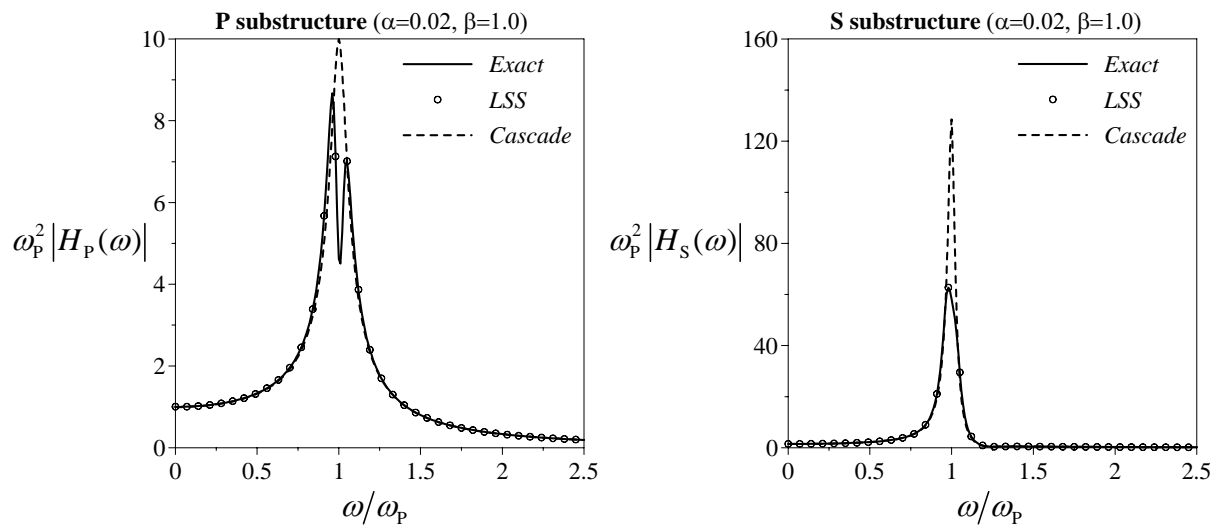
Dimensionless absolute value of the Frequency Response Functions of the 2-DoF combined P-S system with mass ratio $\alpha = 0.02$ and tuning parameter $\beta = 1.0$: P oscillator (left); S oscillator (right).

FIGURE 6

Dimensionless absolute value of the Frequency Response Functions of the 2-DoF combined P-S system with mass ratio $\alpha = 0.10$ and tuning parameters $\beta = 0.5$, 1.0 and 1.5 (log-linear plots): P oscillator (left); S oscillator (right).
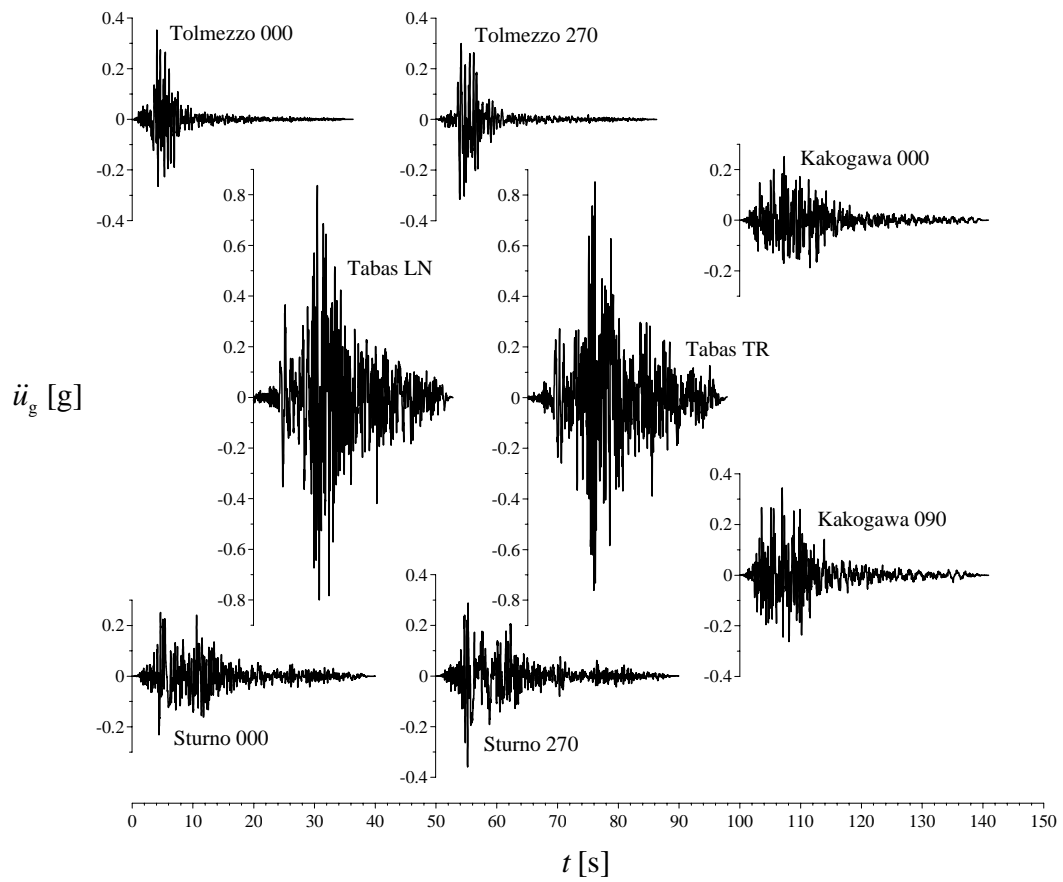
FIGURE 7
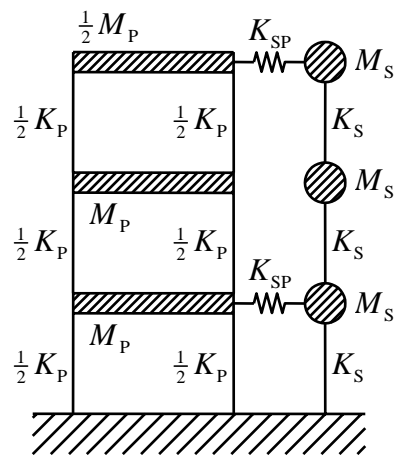
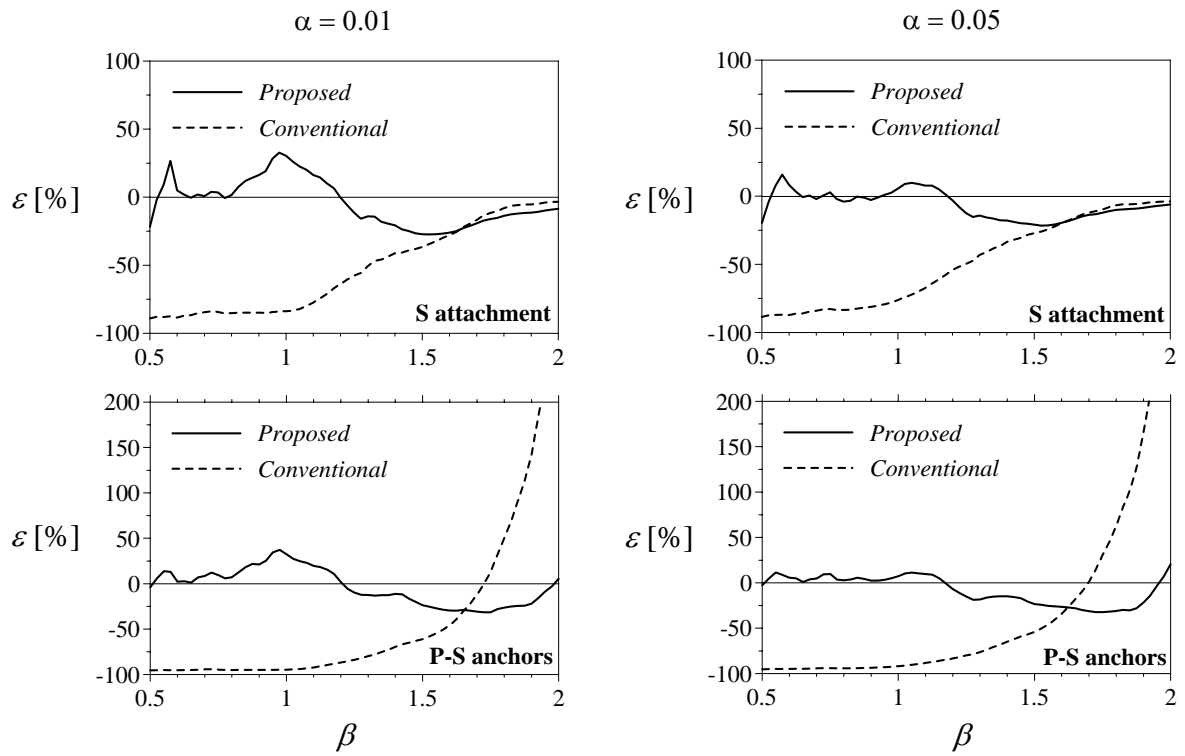Combined P frame-S attachment under investigation.

FIGURE 8
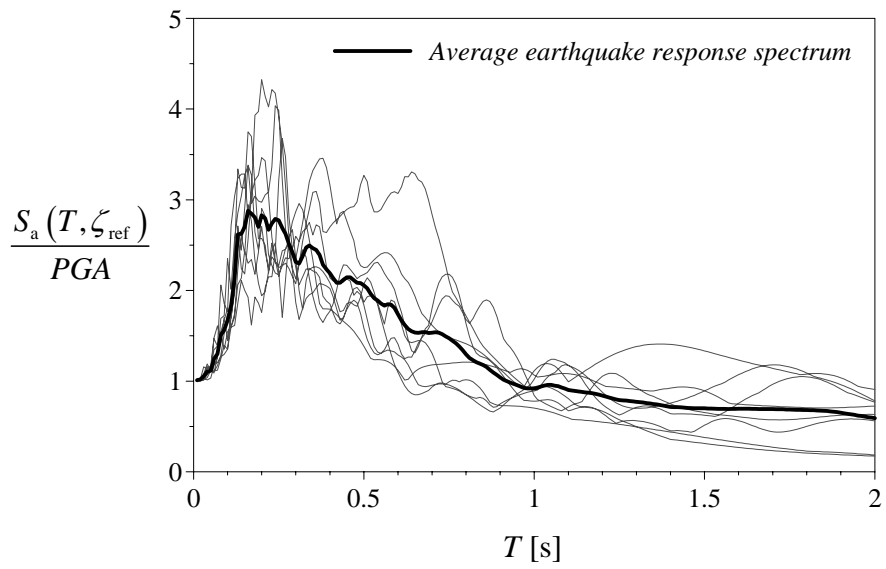
Normalized response spectra for the recorded accelerograms listed in Table 2 (thin lines) and average earthquake response spectrum (thick line).

FIGURE 9

Recorded accelerograms listed in Table 2.

FIGURE 10

Comparison between proposed (solid lines) and conventional (dashed lines) CQC rules for the S attachment (top) and the P-S anchors (bottom); tuning parameter in the range $0.5 \le \beta \le 2.0$; mass ratios $\alpha = 0.01$ (left) and 0.05 (right).